Langmuir

ARTICLE

pubs.acs.org/Langmuir

Photochemical Approach toward Deposition of Gold Nanoparticles on Functionalized Carbon Nanotubes

Farahnaz Begum Lollmahomed and Ravin Narain*

Department of Chemical and Materials Engineering, Alberta Ingenuity Centre for Carbohydrate Science, University of Alberta, Edmonton, AB T6G 2G6, Canada

Supporting Information

ABSTRACT: The development of new methods for the facile synthesis of hybrid nanomaterials is of great importance due to their importance in nanotechnology. In this work, we report a new method to deposit Au nanoparticles on the surface of single-walled carbon nanotubes (SWCNTs). Our approach consists of a one pot synthesis in which Au nanoparticles are generated in the presence of a photoreducing agent (Irgacure-2959) and carboxyl or polymer-functionalized SWCNTs (*f*-SWCNTs). We have observed that when carbon nanotubes are functionalized with polymers containing pendant amino groups, the latter can act as specific nucleation sites for well-dispersed deposition of Au nanoparticles. The surface coverage of the Au nanoparticles can be observed by transmission electron spectroscopy. These observations are compared to that of carboxyl functionalized SWCNTs, in which less surface coverage was observed. The *f*-SWCNT/Au nanocomposites were also characterized by UV−vis, infrared, and Raman spectroscopy and thermogravimetric analysis (TGA). This facile and effective route can be implemented to deposit gold nanoparticles on other surface-functionalized carbon nanotubes.

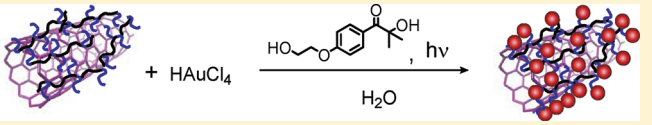

INTRODUCTION

Carbon nanotubes (CNTs) have exceptional mechanical, thermal, and electronic properties that make them unique for applications in various fields such as electronics, catalysis, and medicine. The ease by which their surface can be chemically modified by doping or grafting makes them a desirable platform for various applications. In recent years, nanocomposites in which the noble metal nanoparticles are attached to or deposited on the CNTs have generated considerable interest because they constitute highly promising materials for widespread applications in catalysis (fuel/electrochemical cells or heterogeneous catalysis) and nanotechnology.[1,2] Applications of CNT/noble metal nanocomposites rely on their facile synthesis and on safeguarding the inherent properties of both the CNTs and the noble metal nanoparticles. Considerable research efforts have been directed toward the development of methods to synthesize these nanocomposites. Two main strategies have been employed: (1) naked (that is, without any stabilizing group) metal nanoparticles are deposited directly on the surface of the CNTs, and (2) functionalized nanoparticles are attached to the surface of the CNTs.[3] Among the methods employed to directly deposit naked metal nanoparticles on CNTs are electrodeposition,[4−6] ultrasonication,[7] electroless plating,[8] thermal evaporation,[9] and chemical vapor deposition.[10] One of the limitations of these approaches is that they usually require more sophisticated instrumentation and long reaction time.

Colloidal gold (Au) nanoparticles are of immense scientific interest because of their important utility in biotechnology, diagnostic imaging, and material science due to their high chemical stability, biocompatibility, electrochemical, and optical properties.[11−13] Several studies have been reported on ways for the deposition of Au nanoparticles on CNTs by solution phase synthesis. Choi et al. reported the direct deposition of Au nanoparticles on the walls of single-walled carbon nanotubes (SWCNTs) by the redox reaction between Au^{3+} ions and SWCNTs in a mixture of ethanol and water (1:1).[14] Tzitzios et al. described the deposition of Au nanoparticles on SWCNT surfaces by the reduction of $HAuCl_4$ using polyethylene glycol-200 as reducing agent in DMF.[15] They then covered the surface of the Au nanoparticles with oleylamine to make the composite dispersible in organic solvent. Au nanoparticles have also been linked to CNTs through covalent or electrostatic bonding. In a study, Zanella et al. reacted carboxylated multiwalled carbon nanotubes (MWCNTs) with aminothiols to form amide bonds. Au nanoparticles were then capped to the terminal thiol groups through the Au−S linkage.[16] Hu et al. has demonstrated that Au nanoparticles can be deposited on multiple-walled CNTs functionalized with polyethyleneimine.[17] Recently, Ismaili et al. reported the attachment of functionalized Au nanoparticles to CNT surfaces through a photoinitiated carbene addition reaction.[18]

Wang et al. reported that electrodes consisting of Au/MWCNTs can be used as glucose biosensors when the enzyme glucose oxidase is immobilized on its surface.[10] Recently, a great deal of attention has been paid to noninvasive photothermal therapy for the selective treatment of tumor cells. Both CNTs and Au nanoparticles absorb radiation in the near-infrared

Received: July 4, 2011
Revised: August 23, 2011
Published: August 31, 2011

Scheme 1. Chemical Structures of Monomers, Chain Transfer Agent, and Free Radical Initiator Used in This Study

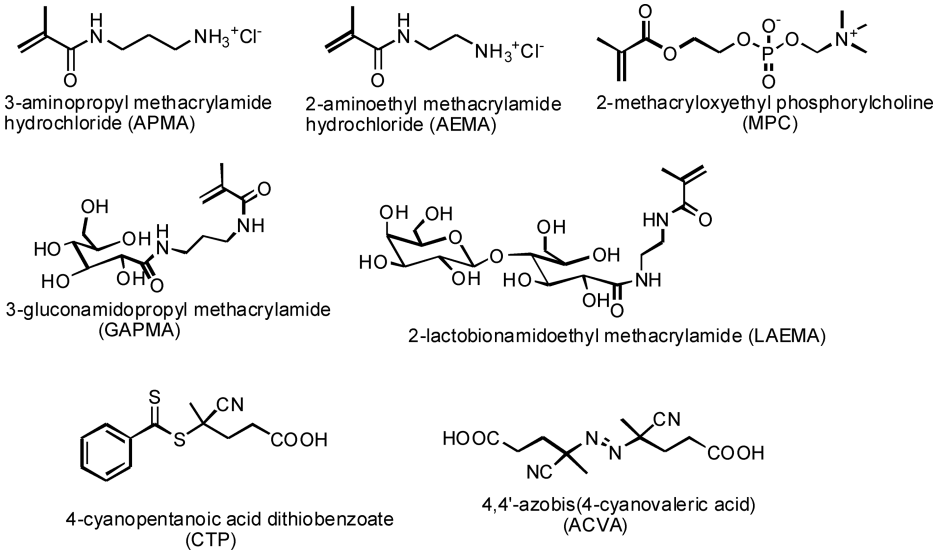

spectrum, where biological systems are transparent. The radiation that is absorbed by these nanomaterials is converted efficiently into heat, causing destruction of surrounding cells. Several groups have reported the efficiency of Au nanoparticles or CNT systems in causing cell destruction of tumor cells after exposure to IR radiation.[19−22] We hypothesized that a nanohybrid material incorporating both Au and CNTs could exhibit enhanced photothermal therapeutic capabilities. In addition, if we surface-functionalized the SWCNT with a biocompatible polymer, this could lead to increased water solubility and reduced cytotoxicity of the system. Furthermore, if we incorporate a cationic moiety in the polymer, this will make it capable of binding and condensing DNA. Ahmed et al. have reported that carbon nanotubes or Au nanoparticles surface functionalized with cationic glycopolymers are efficient gene delivery vectors to mammalian cells and exhibit low cytotoxicity.[23,24] Glycopolymers have been extensively investigated in our group in view of their wide potential applications in the biomedical field, especially in gene delivery and molecular recognition. We thus envisaged that if we functionalize carbon nanotubes with cationic glycopolymers and incorporate Au nanoparticles, these could lead to new hybrid nanomaterials with interesting therapeutic features.

Ahmed et al. have shown that photochemical reduction of hydrogen tetrachloroaurate(III) trihydrate in the presence of glycopolymers containing pendant amine groups leads to the formation of spherical Au nanoparticles that are stable in solution for weeks.[23] We anticipate that, when used to functionalize CNTs, these glycopolymers with pendant amine groups can similarly stabilize Au nanoparticles. In this way, CNTs with well-dispersed deposits of Au nanoparticles can be prepared. To the best of our knowledge, no previous studies have explored the direct attachment of naked gold nanoparticles to polymer-functionalized carbon nanotubes by a photochemical method. Herein, we describe a novel and simple method to directly deposit gold nanoparticles on functionalized surfaces of SWCNTs using a photochemical approach. Our results show that when carbon nanotubes are functionalized with polymers containing several pendant amino groups, deposition of Au nanoparticles is observed.

EXPERIMENTAL SECTION

Materials. Carboxyl-functionalized SWCNTs (SWCNT-COOH), containing carboxyl groups (1.5−3 atom %) were purchased from Carbon Solutions, Inc. and used as received. 4,4′-Azobis(4-cyanovaleric acid) (ACVA, 97%), *N*-hydroxysuccinimide (NHS), *N*-ethyl-*N*′-(3-dimethylaminopropyl)carbodiimide (EDC), 2-(*N*-morpholino) ethanesulfonic acid (MES), hydrogen tetrachloroaurate(III) trihydrate, and hexadecyltrimethylammonium bromide (CTAB) were purchased from Sigma-Aldrich and used as received. Photoreducing agent, Irgacure-2959, was obtained from Ciba Chemicals Inc. *N*,*N*′-Dimethylformamide (DMF) and acetone were purchased from Caledon Chemicals and used as received. The chain transfer agent, 4-cyanopentanoic acid dithiobenzoate (CTP), was synthesized as previously described.[25] 2-Aminoethyl methacrylamide hydrochloride (AEMA), 3-aminopropyl methacrylamide hydrochloride (APMA), 3-gluconamidopropyl methacrylamide (GAPMA), and 2-lactobionamidoethyl methacrylamide (LAEMA) were synthesized according to previous methodologies.[26,27]

Instrumentation. ^{1}H NMR spectra of the monomers and polymers were recorded on a Varian 500 MHz spectrometer using D_2O as solvent. The number average molecular weight (M_n) and polydispersity (M_w/M_n) were determined with respect to Pullulan standards (M_w = 5900−788 000 g mol^{-1}) at room temperature via a Viscotek model 250 dual detector (refractometer/viscometer), using aqueous eluents (0.5 M sodium acetate and 0.5 M acetic acid) at a flow rate of 1.0 mL/min. Two Waters Ultrahydrogel linear WAT011545 columns (10 μm, 7.8 × 300 mm column) were used. Sonication was achieved at the high sonic power mode in an ultrasonic bath (VWR-B2500A-MTH). Photochemical reactions were performed in a Luzchem photoreactor (LZC-4 V model) equipped with four (at the top) and five (on the side) UVA (350 nm) lamps. Transmission electron microscopy (TEM) images were obtained at an accelerating voltage of 80 kV on a Philips/FEI (Morgagni) transmission electron microscope equipped with a CCD camera. TEM samples were prepared by casting a drop of the samples on a 400-mesh carbon-coated copper grid (Ultrathin carbon Type-A; nominal thickness 3−4 nm, Ted Pella, Inc., Redding, CA). TEM images of *f*-SWCNTs were obtained as negatively stained preparations by placing samples in phosphotungstic acid for 1 h. Fourier transform infrared (FTIR) spectra were acquired on a FT-IR Nicolet 8700 spectrometer with PEM (Nicolet-Thermo). UV−vis absorption spectra

of an aqueous solution of Au nanoparticles and *f*-SWCNT/Au nanocomposites were recorded from 300 to 1100 nm on a Jasco V-630 spectrophotometer. Thermogravimetric analysis (TGA) was performed on a SDT Q600 model from TA Instruments, Inc. in alumina pans with a heating rate of 10 °C min^{-1} under air. Prior to analysis by TGA, and IR and Raman spectroscopy, the *f*-SWCNT and *f*-SWCNT/Au nanocomposites were washed thoroughly with water to remove unreacted materials and freeze-dried (FreeZone 2.5, Labconco Corporation, Kansas City, MO). Raman spectroscopy was performed at an excitation wavelength of 532 nm on a Thermo Nicolet Almega XR Raman microscope (with a 50× objective lens).

Methods. *Synthesis of Glycopolymers by RAFT Polymerization Process.* Statistical polymers were synthesized by conventional reversible addition−fragmentation chain transfer (RAFT) radical polymerization, as described elsewhere.[28] The structures of the monomers, RAFT chain transfer agent, and radical initiator used in this work are shown in Scheme 1. A typical procedure for the synthesis of statistical copolymers is as follows: a solution containing ACVA as free radical initiator and CTP as the RAFT chain transfer agent in DMF were placed in a test tube together with aqueous solutions of the monomer(s). The ACVA to CTP mole ratio was maintained to 1:2 while the ratio of volume of water to DMF was kept to 4:1. CTP has previously been reported to give a good control on the polymerization of glycopolymers.[28] The reaction mixture was degassed under a stream of nitrogen for 30 min and then heated at 70 °C with constant stirring for 20 h to afford a pale pink viscous solution of the desired polymer. The polymers were precipitated in acetone, washed several times with same solvent, and dried under vacuum at 25 °C. The samples were then analyzed by aqueous GPC and ^{1}H NMR spectroscopy (D_2O) to determine the molecular mass distribution, polydispersity indices, and relative compositions. Synthetic procedures for each polymer are described in detailed in the Supporting Information.

Functionalization of SWCNT with Cationic Glycopolymers. A typical procedure for the functionalization of SWCNT with the cationic polymers (for e.g. p($APMA_{16}$-*st*-$GAPMA_{27}$)) is as follows: SWCNT-COOH (20 mg, containing 0.1 mmol of carboxyl group) was sonicated for 20 min in distilled water (3 mL) and then a 5 mL solution of EDC (38 mg, 0.2 mmol) and NHS (23 mg, 0.2 mmol) in MES buffer (pH ∼ 6) was added to it. The reaction mixture was sonicated for 5 h. After that time, a basic solution (pH = 7.5) of the polymer (150 mg, 5 mL, 0.2 mmol) was added to the mixture and it was sonicated for further 5 h. After that time, the functionalized carbon nanotubes were purified through repeated centrifugation and washing with distilled water to remove any unbound polymer. Finally, the deposits were combined and lyophilized. The resulting surface functionalized carbon nanotubes were characterized by Raman and FTIR spectroscopy and TEM and TGA analyses.

Deposition of Spherical Au Nanoparticles on SWCNT-COOH. An aqueous solution of hydrogen tetrachloroaurate(III) trihydrate (2 mg/mL), Irgacure-2959 (23.94 mg dissolved in 0.25 mL of MeOH and 0.75 mL of water), and SWCNT-COOH (0.25 mg dispersed by sonication in 2 mL of water) were combined in a 20 mL pyrex scintillation vial. The mixture was irradiated for 10 min with nine UVA (350 nm) lamps in a Luzchem photoreactor. The SWCNTs were tinted cherry-red after the reaction. When the experiment was performed with 1 mg of SWCNT-COOH, it was hard to differentiate between the UV−vis spectra recorded before and after the reaction because the carbon nanotubes exhibit a broad absorption band in the UV range 400−600 nm.

Synthesis of p(MPC_{57}-st-$AEMA_{51}$)-SWCNT/Au Nanocomposites. A representative procedure is as follows: briefly, an aqueous solution of hydrogen tetrachloroaurate(III) trihydrate (2 mg/mL), p(MPC_{57}-*st*-$AEMA_{51}$)-SWCNT (4 mg dispersed in 2 mL distilled water), Irgacure-2959 (23.94 mg dissolved in 0.25 mL of MeOH and 0.75 mL of water) were combined in a 20 mL pyrex scintillation vial and irradiated with continuous stirring for 10 min with nine UVA (350 nm) lamps in a Luzchem photoreactor. After that time, a cherry-red well-dispersed solution was obtained.

Table 1. Molecular Weight Distribution (M_n) and Polydispersity Indices (M_n/M_w) of Statistical Glycopolymers[a]

polymer (targeted)	polymer (experimental)	M_n (g mol^{-1})	M_w/M_n
P($AEMA_{40}$-*st*-MPC_{60})	P($AEMA_{51}$-*st*-MPC_{57})	25 302	1.21
P($AEMA_{30}$-*st*-$GAPMA_{30}$)	P($AEMA_{7}$-*st*-$GAPMA_{16}$)	6256	1.19
P($AEMA_{30}$-*st*-$LAEMA_{30}$)	P($AEMA_{10}$-*st*-$LAEMA_{15}$)	8657	1.17
P($AEMA_{62}$)	P($AEMA_{60}$)	9800	1.20
P($APMA_{30}$-*st*-$GAPMA_{30}$)	P($APMA_{16}$-*st*-$GAPMA_{27}$)	11 523	1.18

[a] As determined by aqueous gel permeation chromatography, calibrated with seven near-monodisperse Pullulan standards (M_w = 5900−788 000 g mol^{-1}) with mobile phase of 0.5 M sodium acetate/acetic acid buffer.

RESULTS AND DISCUSSION

A series of statistical polymers bearing pendant amino groups was prepared by using monomers, 3-aminopropyl methacrylate hydrochloride (APMA), 2-aminoethyl methacrylate hydrochloride (AEMA), 3-gluconamidopropyl methacrylate hydrochloride (GAPMA), 2-lactobionamidoethyl methacrylate hydrochloride (LAEMA), and 2-methacryloyloxyethyl phosphorylcholine (MPC) by the RAFT process as previously described by Deng et al.[28] The molecular weight distributions (M_n) of the statistical copolymers were determined by gel permeation chromatography (GPC) analysis. The results show that polymers are near-monodisperse, with polydispersity indices (M_w/M_n) < 1.2. The relative compositions of each monomer in the copolymer were subsequently determined by ^{1}H NMR spectroscopy. The molecular weights distributions and polydispersity indices of the polymers synthesized are summarized in Table 1.

One of the most common approaches for functionalizing carbon nanotubes involves the introduction of carboxylic acid groups onto their surfaces via acid treatment.[29] These carboxylic groups can be used to covalently attach materials such as polymers,[24] oligonucleotides,[30] and proteins[31] to the carbon nanotubes. The SWCNT-COOH were first sonicated to disperse them into water. Then the carboxyl groups on the surface were activated by the addition of 1-ethyl-3(3-dimethylaminopropyl)carbodiimide (EDC)-*N*-hydroxysuccinimide (NHS) reagents at pH 6 (0.1 M MES buffer). The polymers (pH ∼ 7.5) were then added to the activated SWCNTs, leading to the formation of surface polymer-functionalized SWCNTs (Scheme 2). Evidence for the successful functionalization of the SWCNTs was obtained from TEM analysis, and IR and Raman spectroscopies. Representative TEM images of the polymer-functionalized SWCNTs are shown in Figure S1 in the Supporting Information. The *f*-SWCNTs appear to be aggregated into bundles, and the presence of impurities from the purchased SWCNTs appears as black spots. However, the images reveal less bundled materials than what is typically found for SWCNT-COOH. In solution, the *f*-SWCNTs were well dispersed at concentrations ranging from 4 to 7 mg/mL.

The FTIR spectra (KBr) measured in the solid state for the SWCNT-COOH and glycopolymer surface-functionalized carbon nanotubes are shown in Figure 1. In the case of the SWCNT-COOH, a band at 1630 cm^{-1} due to the symmetric C═O

Scheme 2. Functionalization of SWCNT with Cationic Glycopolymers via EDC/NHS Coupling in Aqueous Solution

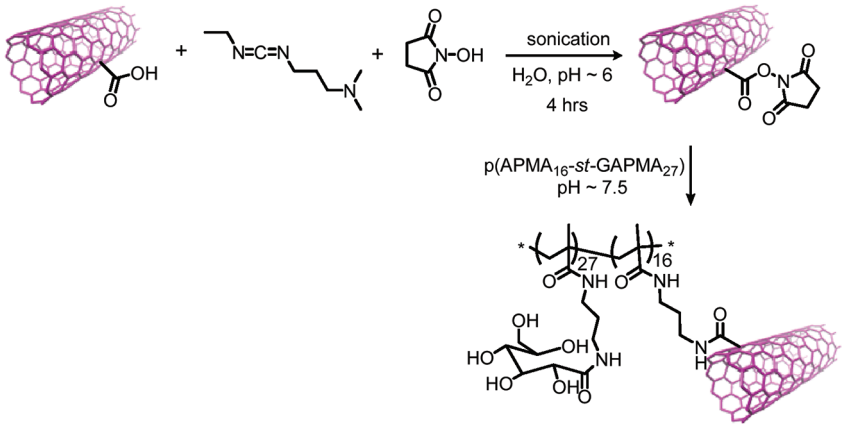

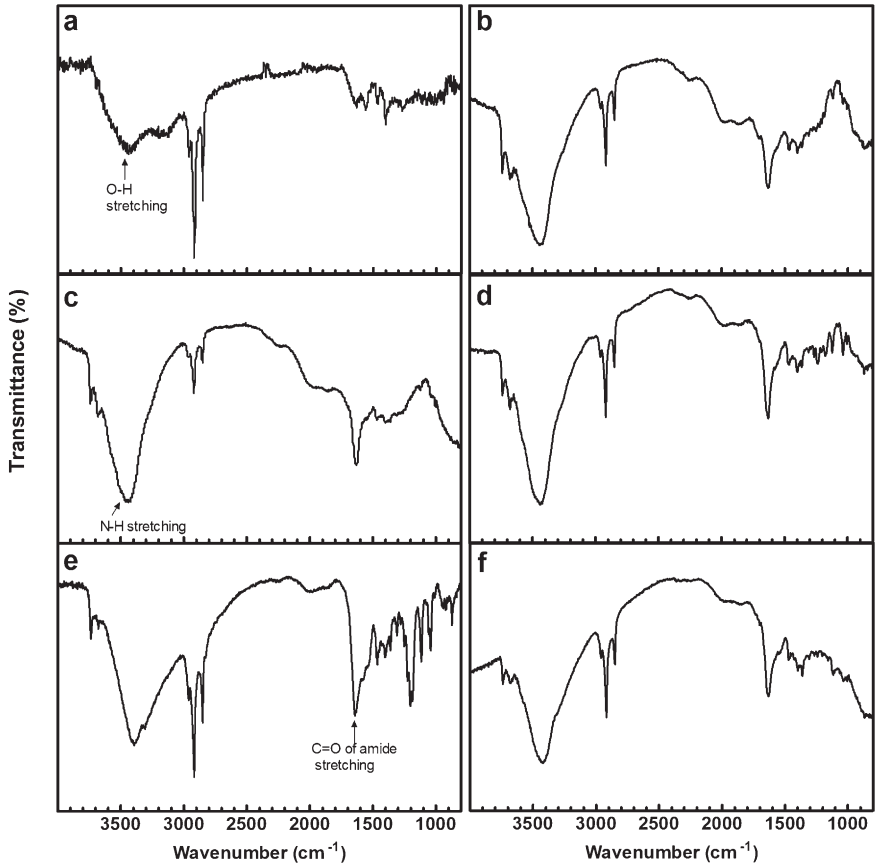

Figure 1. FTIR spectra (KBr) of (a) SWCNT-COOH, (b) p($APMA_{16}$-*st*-$GAPMA_{27}$)-SWCNT, (c) p($AEMA_7$-*st*-$GAPMA_{16}$)-SWCNT, (d) p($AEMA_{51}$-*st*-MPC_{57})-SWCNT, (e) p($AEMA_{60}$)-SWCNT, and (f) p($AEMA_{10}$-*st*-$LAEMA_{15}$)-SWCNT measured in the solid state.

stretching of carboxylic group is observed. The absorption peaks at 2920 and 2850 cm^{-1} characteristic of the stretching mode of C−H stretching vibration can be observed in all four samples. Upon functionalization, strong absorption bands in the wavenumber region of 3400 cm^{-1} characteristic of N−H stretching frequency of primary amines were observed for all four *f*-SWCNTs. In addition, an enhancement in the intensity of the band at ~1623 cm^{-1} is observed, and this is attributable to the C═O stretching of amide.

The Raman spectra for the SWCNT-COOH and the *f*-SWCNTs exhibit several radial breathing modes in the range of 160−180 cm^{-1} typical for carbon nanotubes (Figure S2, Supporting Information). The Raman spectrum of the SWCNT-COOH shows a G band (sp^2 tangential mode) at 1570 cm^{-1}; this band appears at 1580−1590 cm^{-1} in the *f*-SWCNTs. The D band which is due to sp^3 hybridized carbons appears at 1290−1300 cm^{-1}. The second order modes (G′-band) for all the SWCNTs appear at ~2640 cm^{-1}. The close similarity in the

dx.doi.org/10.1021/la2025268 |*Langmuir* 2011, 27, 12642–12649

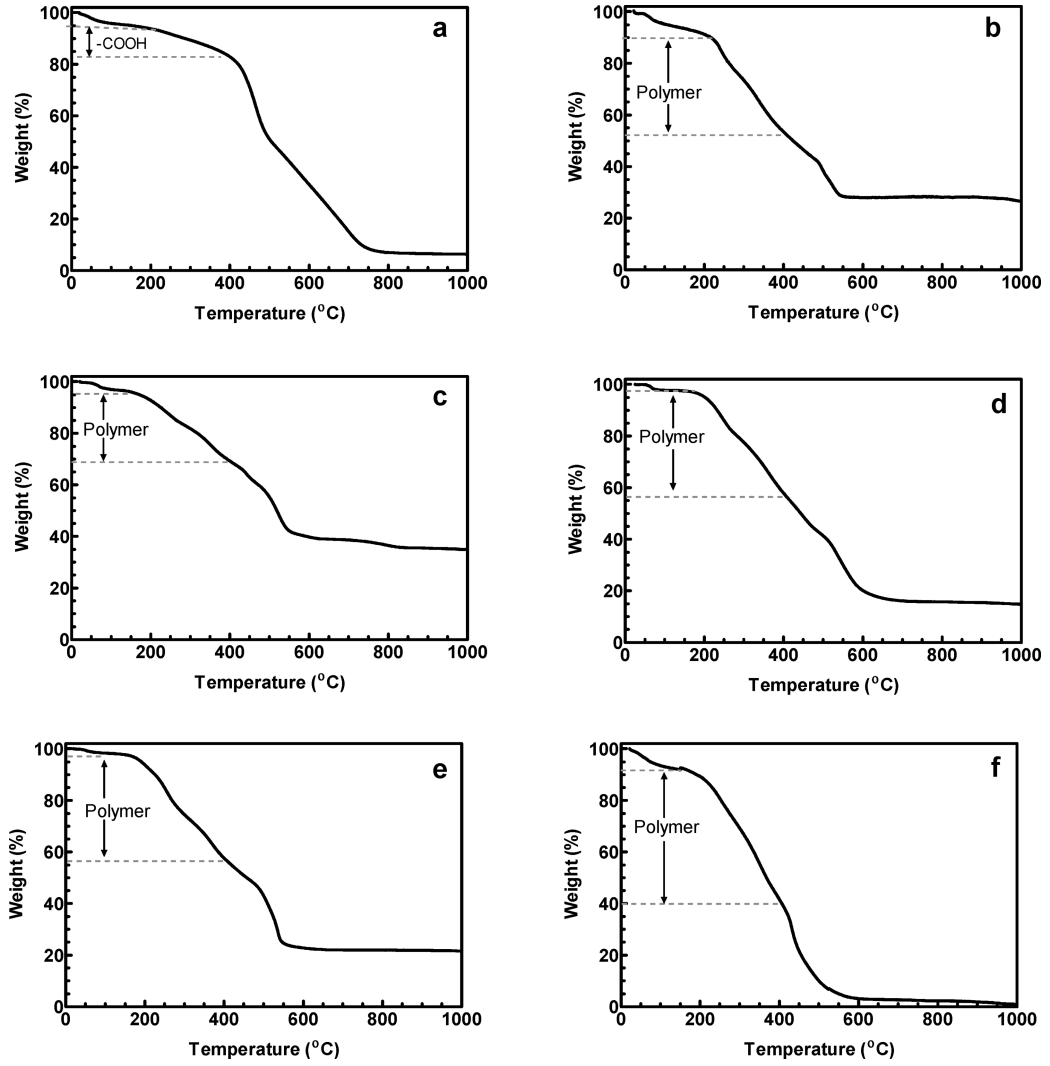

Figure 2. TGA curves of *f*-SWCNT recorded in air (ramp of 10 °C min^{-1} from 25 to 1000 °C) for (a) SWCNT-COOH, (b) p($APMA_{16}$-*st*-$GAPMA_{27}$)-SWCNT, (c) p($AEMA_7$-*st*-$GAPMA_{16}$)-SWCNT, (d) p($AEMA_{51}$-*st*-MPC_{57})-SWCNT, (e) p($AEMA_{60}$)-SWCNT, and (f) p($AEMA_{10}$-*st*-$LAEMA_{15}$)-SWCNT.

Raman shifts observed for the SWCNT-COOH and the *f*-SWCNTs indicates that the sidewall of the single-walled carbon nanotubes is not changed after the functionalization with the polymers, consistent with what was previously observed by Narain et al.[32]

To determine the extent of sidewall functionalization on the carbon nanotubes, TGA analysis was performed in air. Figure 2 shows a comparison of the percent weight loss of the SWCNT-COOH and the other five polymer-functionalized SWCNTs during the calcination in air. The differential thermogravimetric (DTG) curves display several weight-loss peaks (see Figure S3 in the Supporting Information). The weight loss below 150 °C was assigned to the loss of adsorbed water in the samples. The SWCNT-COOH undergo a weight loss of about 8% in the 154−400 °C range, corresponding to the loss of the carboxyl groups. A sharper weight loss is observed from 400 to 750 °C, attributable to decomposition of the SWCNTs due to oxidation by air. The shapes of the percent weight loss curves corresponding to the other functionalized SWCNTs exhibit a distinctive degradation profile similar to that of SWCNT-COOH. In all cases, a drastic weight loss is observed between 200 and 400 °C and is attributed to the thermal decomposition of the polymers present on the surface of the SWCNTs. The corresponding DTG shows multiple peaks characteristic of thermal degradation of polymers which are typically complex. The total weight loss (wt %) and transition temperatures observed for the SWCNT-COOH and polymer surface-functionalized SWCNTs are summarized in Table S1 (Supporting Information). The overall percent weight losses observed were 42, 27, 50, 43, and 38 for carbon nanotubes surface-functionalized with p($AEMA_{51}$-*st*-MPC_{57}), p($AEMA_7$-*st*-$GAPMA_{16}$), p($AEMA_{10}$-*st*-$LAEMA_{15}$), p$(AEMA)_{60}$, and p($APMA_{16}$-*st*-$GAPMA_{27}$), respectively.

Gold nanoparticles are commonly produced in solution by the chemical reduction of metal salts in the presence of a stabilizer. A number of ways have been used to prepare Au nanoparticles including Turkevich method (citrate reduction),[33] Brust−Schiffrin method of two phase synthesis involving reduction with borohydride,[34] and seeding growth using ascorbic acid.[35] McGilvray et al. described the photochemical synthesis of gold nanoparticles in the presence of 1-[4-(2-hydroxyethoxy)phenyl]-2-hydroxy-2-methyl-1-propane-1-one (Irgacure-2959) as photoreducing agent.[36] Furthermore,

Scheme 3. Schematic Showing Deposition of Au Nanoparticle on the Functionalized Surface of SWCNTs upon UV−Vis Irradiation[a]

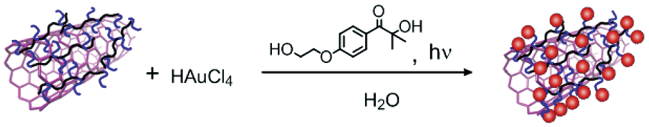

[a] The pendant amine groups are represented by blue.

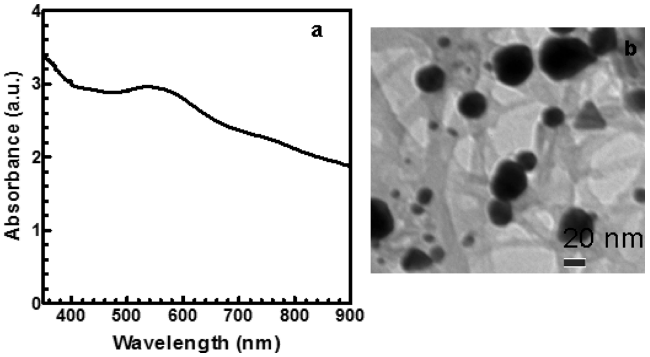

Figure 3. (a) UV−vis absorption spectrum of an aqueous mixture of SWCNT-COOH/Au nanocomposites. (b) TEM micrograph showing of Au nanoparticles deposited on SWCNT-COOH.

Ahmed et al. reported the photochemical synthesis of Au nanoparticles in the presence of glycopolymers containing pendant amino groups.[23] It was suggested that the amine groups can stabilize Au nanoparticles by the formation of N−Au linkage (6 kcal/mol).[37] Similarly, here we anticipate that, when attached on the surface of the carbon nanotubes, glycopolymers containing pendant amine groups can bind to Au nanoparticles. In this work, deposition of Au nanoparticles was achieved by the photochemical reduction of Au^{3+} to Au in the presence of Irgacure-2959 as photoreducing agent (Scheme 3). In our experiments, it was necessary to increase the concentration of the Irgacure-2959 such that it is the main UV-absorber at 350 nm, given that the functionalized carbon nanotubes also absorb at this wavelength (see Figure S4, Supporting Information). This ensures that enough ketyl radicals are produced to reduce Au^{3+}. The reaction mixture was irradiated with UVA lamps (λ = 350 nm) for a total of 10 min, after which time the UV−vis absorption spectra of the products were recorded. First, the deposition of Au nanoparticles on carboxyl functionalized carbon nanotubes (SWCNT-COOH) was investigated. SWCNT-COOH was first dispersed in water by sonication. An aqueous mixture containing SWCNT-COOH, hydrogen tetrachloroaurate-(III) trihydrate, and Irgacure-2959 as photochemical initiator was irradiated at 350 nm for 10 min. Figure 3a depicts the UV−vis absorption spectrum recorded for the resulting mixture obtained after 10 min irradiation of an aqueous solution containing SWCNT-COOH, hydrogen tetrachloroaurate(III) trihydrate, and Irgacure-2959. The new absorption band at 530 nm can be attributed to the plasmon resonance absorption band of spherical Au nanoparticles. The samples were analyzed by TEM after repeated centrifugation and washing with distilled water. Figure 3b shows TEM micrographs of Au nanoparticles formed in the presence of SWCNT-COOH. Random sizes of Au nanoparticles are observed. Nucleation most likely takes place at the carboxylic or defect sites present on the surface;[38] however, the high polydispersity suggests poor stabilization of the nanoparticles. It is observed that the SWCNT-COOH/Au nanocomposites sink to the bottom of the solution a few minutes after the reaction.

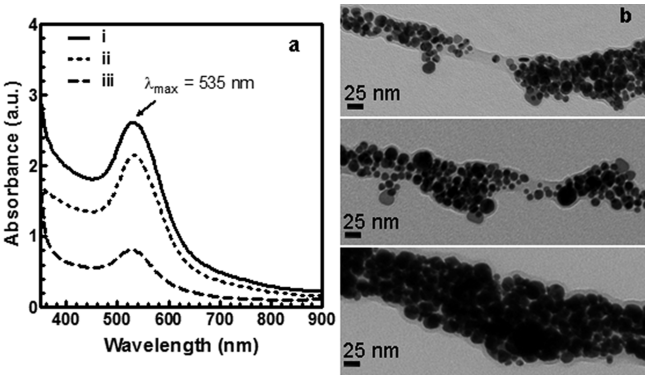

Figure 4. (a) UV−vis absorption spectra recorded after 10 min irradiation of an aqueous mixture containing p($AEMA_{51}$-*st*-MPC_{57})-SWCNT, hydrogen tetrachloroaurate(III) trihydrate, and Irgacure-2959 (i) product from reaction mixture; (ii) deposit after centrifugation; and (iii) supernatant from centrifugation. (b) TEM micrographs showing Au nanoparticles deposited on p($AEMA_{51}$-*st*-MPC_{57})-SWCNTs.

Irradiation of a mixture of p($AEMA_{51}$-*st*-MPC_{57})SWCNT, hydrogen tetrachloroaurate(III) trihydrate, and Irgacure-2959 for 10 min afforded a cherry-red solution that is stable without flocculation for months in the dark at room temperature. The UV−vis absorption spectrum of the reaction mixture showed a narrow absorption band with an absorption maximum at 535 nm. This indicates the presence of spherical Au nanoparticles and the absence of aggregates. This is in agreement with Hu et al. who also observed a narrow absorption spectrum at ∼550 nm for a solution of Au nanoparticles deposited on carbon nanotubes functionalized with polyethyleneimine.[17] The p($AEMA_{51}$-*st*-MPC_{57})SWCNT/Au nanocomposite solution was centrifuged at 8000 rpm for 10 min at 20 °C. The UV−vis spectra of the centrifuged material (the deposit and supernatant liquid) and original mixture are similar (Figure 4a). The fact that little loss of Au nanoparticles is observed after the sample was washed several times with water indicates strong interactions between the Au nanoparticles and the SWCNTs. TEM analysis of the reaction mixture revealed that spherical Au nanoparticles with an average diameter of about 5−25 nm are dispersed entirely on the surface of the functionalized SWCNT (Figure 4b). These results suggest that Au nanoparticles are stabilized by the p(MPC_{57}-*st*-$AEMA_{51}$) polymer chains attached on the surface of the CNTs. In addition, the nearly uniform coverage of Au nanoparticles indicates that functional groups are throughout the length of the CNTs. It is also noted that the Au nanoparticles are attached close to the surface of the carbon nanotubes. Interestingly, less surface coverage was also observed in some areas, most likely indicating areas with lower grafting density. There is a remarkable difference between the extent of Au nanoparticles deposition on the SWCNT-COOH and that of the p($AEMA_{51}$-*st*-MPC_{57})-SWCNT. In the latter case, more sites are available for nucleation on the polymers. In addition, the near monodispersity of the particles suggests that surface-grafted polymers provide good stabilization to the Au nanoparticles. It is noted that the UV−vis absorption spectrum recorded for p($AEMA_{51}$-*st*-MPC_{57})-SWCNT/Au nanocomposites is similar to the one recorded for an aqueous solution of the Au nanoparticles photochemically generated in the presence of the free polymer only

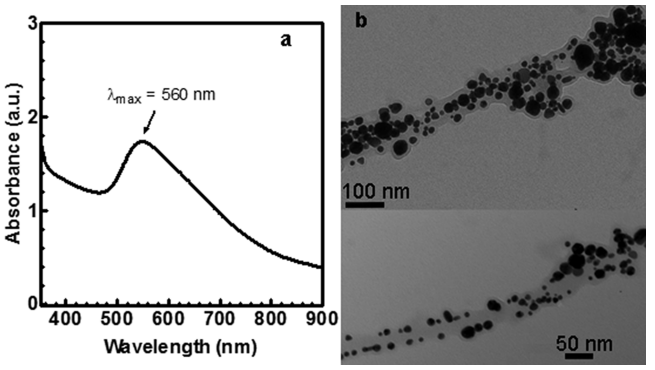

Figure 5. (a) UV−vis absorption spectrum obtained after 10 min irradiation of an aqueous mixture containing p(AEMA$_7$-*st*-GAPMA$_{16}$)-SWCNTs, hydrogen tetrachloroaurate(III) trihydrate, and Irgacure-2959. (b) TEM micrographs showing deposits of Au nanoparticles on the surface of p(AEMA$_7$-*st*-GAPMA$_{16}$)-SWCNTs.

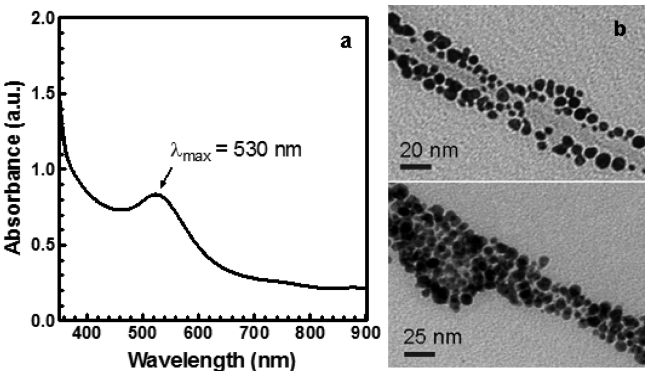

Figure 6. (a) UV−vis absorption spectrum recorded after 10 min irradiation of an aqueous mixture containing p(AEMA$_{60}$)-SWCNTs, hydrogen tetrachloroaurate(III) trihydrate and Irgacure-2959. (b) TEM micrographs showing Au nanoparticles deposited on the surface of p(AEMA$_{60}$)-SWCNTs.

(λ_{max} = 530 nm; see Figure S5 in the Supporting Information). These observations indicate that the Au nanoparticles are of similar size. The fact that these nanocomposites are easily dispersed in water is an important feature that allows their purification for further applications in the biomedical field.

When p(AEMA$_7$-*st*-GAPMA$_{16}$)-SWCNT was used, an absorption spectrum with λ_{max} = 560 nm and considerable tailing toward longer wavelength was recorded after 10 min of irradiation (Figure 5a). The Au nanoparticles formed are highly polydisperse with sizes ranging from 10 to 100 nm. Moreover, relatively less surface coverage of Au nanoparticles as in the case of p(AEMA$_{51}$-*st*-MPC$_{57}$)-SWCNTs was observed (Figure 5b). TGA analyses show that the grafting densities of the polymer on the two surfaces are almost same. These observations can be attributed to the less amount of the amino group present on the attached polymer chains.

When p(AEMA$_{10}$-*st*-LAEMA$_{15}$)-SWCNTs was used for the experiment, after 10 min irradiation, the reaction mixture appeared pale purple. The UV−vis absorption spectrum of the reaction mixture recorded after 10 min of irradiation showed a new absorption band at λ_{max} = 550 nm which is attributed to the plasmon resonance of spherical Au nanoparticles (Figure S6a, Supporting Information). This slight red shift indicates larger size of particles, which is supported by TEM analysis of the sample. TEM micrographs show Au nanoparticles of sizes (20−30 nm) on the surface of the CNTs (Figure S6b, Supporting Information)

When Au nanoparticles were generated in the presence of p(APMA$_{16}$-*st*-GAPMA$_{27}$)-SWCNTs, black aggregates in a pale blue solution were obtained. The UV−vis absorption spectrum of that mixture shows a broad absorption band in the region of 500−900 nm (Figure S7a, Supporting Information). TEM micrographs show deposition of Au nanoparticles on the surface of the CNTs (Figure S7b, Supporting Information). Large aggregates and high polydispersity in the Au nanoparticles are observed.

Given that a uniform dispersion of Au nanoparticles is observed only with high amine component of the polymer, we thought of investigating the deposition and monodispersity of Au nanoparticles on highly substituted amine homopolymer functionalized SWCNTs. For that purpose, p(AEMA$_{60}$) which is a homopolymer bearing on average 60 amino groups per polymer chain was chosen. We also wanted to investigate whether it will lead to an increase in deposition and monodispersity of Au nanoparticles. The UV−vis absorption spectrum recorded for the product shows an absorption band centered at 530 nm, consistent with the formation of spherical Au nanoparticles (Figure 6a). The TEM micrographs show uniform coverage of Au nanoparticles, with average size of 5−20 nm, on the surface of the *f*-SWCNT comparable to that observed with p(AEMA$_{51}$-*st*-MPC$_{57}$)-SWCNT (Figure 6b).

In all the cases, except for p(AEMA$_{51}$-*st*-MPC$_{57}$)-SWCNT and p(AEMA$_{60}$)-SWCNT, sedimentation of the nanocomposites was observed after 1 day. The nanocomposites were robust enough to survive repeated washings in water. The density of the Au nanoparticles assembled on the SWCNT-COOH is sparse as compared to that deposited on polymer-functionalized CNTs showing that carboxyl groups are poor stabilizers for Au nanoparticles.[39] It is observed that the uniformity of the deposition of Au nanoparticles on the SWCNTs is dependent on the number of amino groups present on the SWCNTs' surface. SWCNTs bearing a higher composition of amino groups lead to more uniform dispersion and more stable nanocomposites with respect to flocculation. When the substituents on the SWCNTs are p(AEMA$_{10}$-*st*-LAEMA$_{15}$), p(AEMA$_7$-*st*-GAPMA$_{16}$), and p(APMA$_{16}$-*st*-GAPMA$_{27}$), much less amino groups are available, resulting in decreased stabilization of the Au nanoparticles. Consequently, the Au nanoparticles formed are polydisperse. These results show that a critical amount of amino groups is required for uniform Au deposition.

This direct photochemical approach for depositing Au nanoparticles on the surface of functionalized CNTs is a simple, rapid and effective method, and a large amount of Au can be deposited if the carbon nanotubes are adequately functionalized. However, it is observed that it is rather challenging to control the size, morphology, and percentage of the nanoparticles deposited. There is ongoing work to optimize the conditions such that these parameters can be controlled.

CONCLUSIONS

To summarize, we report the facile synthesis of surface-functionalized SWCNTs/Au nanocomposites by a photochemical method. We have demonstrated that photochemical reduction of hydrogen tetrachloroaurate(III) trihydrate in the presence of Irgacure-2959 and SWCNTs functionalized with amine-containing

polymers leads to heavy coverage of the carbon nanotubes' surfaces by Au nanoparticles. The primary amines present on the polymer chains play a crucial role in the stabilization of the Au nanoparticles and their uniform deposition on the SWCNTs' surface. This simple method can be extended to prepare other noble metal/SWCNTs nanocomposites that can be used in catalysis and nanotechnology. These types of materials can be of significant importance in therapeutic medicine.

■ ASSOCIATED CONTENT

Supporting Information. Detailed synthesis of polymers and functionalized carbon nanotubes. Additional characterization data. This material is available free of charge via the Internet at http://pubs.acs.org.

■ AUTHOR INFORMATION

Corresponding Author

*E-mail: narain@ualberta.ca. Fax: 1 780 492 2881.

■ ACKNOWLEDGMENT

We thank the Natural Sciences and Engineering Research Council of Canada and the Alberta Ingenuity Centre for Carbohydrate Science for financial support for this work.

■ REFERENCES

(1) Eder, D. *Chem. Rev.* **2010**, *110*, 1348–1385.
(2) Wildgoose, G. G.; Banks, C. E.; Compton, R. G. *Small* **2006**, *2*, 182–193.
(3) Georgakilas, V.; Gournis, D.; Tzitzios, V.; Pasquato, L.; Guldi, D. M.; Prato, M. *J. Mater. Chem* **2007**, *17*, 2679–2694.
(4) Quinn, B. M.; Dekker, C.; Lemay, S. G. *J. Am. Chem. Soc.* **2005**, *127*, 6146–6147.
(5) Day, T. M.; Unwin, P. R.; Macpherson, J. V. *Nano Lett.* **2007**, *7*, 51–57.
(6) Franklin, A. D.; Smith, J. T.; Sands, T.; Fisher, T. S.; Choi, K. S.; Janes, D. B. *J. Phys. Chem. C* **2007**, *111*, 13756–13762.
(7) Shi, Y.; Yang, R.; Yuet, P. K. *Carbon* **2009**, *47*, 1146–1151.
(8) Ma, X.; Li, X.; Lun, N.; Wen, S. *Mater. Chem. Phys.* **2006**, *97*, 351–356.
(9) Gingery, D.; Bühlmann, P. *Carbon* **2008**, *46*, 1966–1972.
(10) Wang, S. G.; Zhang, Q.; Wang, R.; Yoon, S. F.; Ahn, J.; Yang, D. J.; Tian, J. Z.; Li, J. Q.; Zhou, Q. *Electrochem. Commun.* **2003**, *5*, 800–803.
(11) Wang, Z.; Ma, L. *Coord. Chem. Rev.* **2009**, *253*, 1607–1618.
(12) Schotz, A.; Reiser, O.; Stark, W. J. *Chem.—Eur. J.* **2010**, *16*, 8950–8967.
(13) Daniel, M. C.; Astruc, D. *Chem. Rev.* **2004**, *104*, 293–346.
(14) Choi, H. C.; Shim, M.; Bangsaruntip, S.; Dai, H. *J. Am. Chem. Soc.* **2002**, *124*, 9058–9059.
(15) Tzitzios, V.; Georgakilas, V.; Oikonomou, E.; Karakassides, M.; Petridis, D. *Carbon* **2006**, *44*, 848–853.
(16) Zanella, R.; Basiuk, E. V.; Santiago, P.; Basiuk, V. A.; Mireles, E.; Puente-Lee, I.; Saniger, J. M. *J. Phys. Chem. B* **2005**, *109*, 16290–16295.
(17) Hu, X.; Wang, T.; Qu, X.; Dong, S. *J. Phys. Chem. B* **2006**, *110*, 853–857.
(18) Ismaili, H.; Lagugné-Labarthet, F.; Workentin, M. S. *Chem. Mater.* **2011**, *23*, 1519–1525.
(19) Kam, N. W. S.; O'Connell, M.; Wisdom, J. A.; Dai, H. *Proc. Natl. Acad. Sci. U.S.A.* **2005**, *102*, 11600–11605.
(20) Chakravarty, P.; Marches, R.; Zimmerman, N. S.; Swafford, A. D. E.; Bajaj, P.; Musselman, I. H.; Pantano, P.; Draper, R. K.; Vitetta, E. S. *Proc. Natl. Acad. Sci. U.S.A.* **2008**, *105*, 8697–8702.
(21) Hirsch, L. R.; Stafford, R. J.; Bankson, J. A.; Sershen, S. R.; Rivera, B.; Price, R. E.; Hazle, J. D.; Halas, N. J.; West, J. L. *Proc. Natl. Acad. Sci. U.S.A.* **2003**, *100*, 13549–13554.
(22) Shao, N.; Lu, S.; Wickstrom, E.; Panchapakesan, B. *Nanotechnology* **2007**, *18*, 315101–315108.
(23) Ahmed, M.; Deng, Z.; Liu, S.; Lafrenie, R.; Kumar, A.; Narain, R. *Bioconjugate Chem.* **2009**, *20*, 2169–2176.
(24) Ahmed, M.; Jiang, X.; Deng, Z.; Narain, R. *Bioconjugate Chem.* **2009**, *20*, 2017–2022.
(25) Mitsukami, Y.; Donovan, M. S.; Lowe, A. B.; McCormick, C. L. *Macromolecules* **2001**, *34*, 2248–2256.
(26) Deng, Z.; Bouchékif, H.; Babooram, K.; Housni, A.; Choytun, N.; Narain, R. *J. Poly. Sci., Part A: Polym. Chem.* **2008**, *46*, 4984–4996.
(27) Deng, Z.; Li, S.; Jiang, X.; Narain, R. *Macromolecules* **2009**, *42*, 6393–6405.
(28) Deng, Z.; Ahmed, M.; Narain, R. *J. Polym. Sci., Part A: Polym. Chem.* **2009**, *47*, 614–627.
(29) Liu, J.; Rinzler, A. G.; Dai, H.; Hafner, J. H.; Bradley, R. K.; Boul, P. J.; Lu, A.; Iverson, T.; Shelimov, K.; Huffman, C. B.; Rodriguez-Macias, F.; Shon, Y. S.; Lee, T. R.; Colbert, D. T.; Smalley, R. E. *Science* **1998**, *280*, 1253–1256.
(30) Baker, S. E.; Cai, W.; Lasseter, T. L.; Weidkamp, K. P.; Hamers, R. J. *Nano Lett.* **2002**, *2*, 1413–1417.
(31) Huang, W.; Taylor, S.; Fu, K.; Lin, Y.; Zhang, D.; Hanks, T. W.; Rao, A. M.; Sun, Y. P. *Nano Lett.* **2002**, *2*, 311–314.
(32) Narain, R.; Housni, A.; Lane, L. *J. Polym. Sci., Part A: Polym. Chem.* **2006**, *44*, 6558–6568.
(33) Turkevich, J.; Stevenson, P. C.; Hillier, J. *Discuss. Faraday Soc.* **1951**, *11*, 55–75.
(34) Brust, M.; Walker, M.; Bethell, D.; Schiffrin, D. J.; Whyman, R. *J. Chem. Soc., Chem. Commun.* **1994**, *7*, 801–802.
(35) Jana, N. R.; Gearheart, L.; Murphy, C. J. *Langmuir* **2001**, *17*, 6782–6786.
(36) McGilvray, K. L.; Decan, M. R.; Wang, D.; Scaiano, J. C. *J. Am. Chem. Soc.* **2006**, *128*, 15980–15981.
(37) Di Felice, R.; Selloni, A. *J. Chem. Phys.* **2004**, *120*, 4906–4914.
(38) Quintana, M.; Ke, X.; Van Tendeloo, G.; Meneghetti, M.; Bittencourt, C.; Prato, M. *ACS Nano* **2010**, *4*, 6105–6113.
(39) Wang, Z.; Tan, B.; Hussain, I.; Schaeffer, N.; Wyatt, M. F.; Brust, M.; Cooper, A. I. *Langmuir* **2007**, *23*, 885–895.